© 2020. Published by The Company of Biologists Ltd | Journal of Experimental Biology (2020) 223, jeb211912. doi:10.1242/jeb.211912

RESEARCH ARTICLE

Disease recovery in bats affected by white-nose syndrome

Nathan W. Fuller[1,*], Liam P. McGuire[1], Evan L. Pannkuk[2], Todd Blute[3], Catherine G. Haase[4], Heather W. Mayberry[5], Thomas S. Risch[6] and Craig K. R. Willis[7]

ABSTRACT

Processes associated with recovery of survivors are understudied components of wildlife infectious diseases. White-nose syndrome (WNS) in bats provides an opportunity to study recovery of disease survivors, understand implications of recovery for individual energetics, and assess the role of survivors in pathogen transmission. We documented temporal patterns of recovery from WNS in little brown bats (*Myotis lucifugus*) following hibernation to test the hypotheses that: (1) recovery of wing structure from WNS matches a rapid time scale (i.e. approximately 30 days) suggested by data from free-ranging bats; (2) torpor expression plays a role in recovery; (3) wing physiological function returns to normal alongside structural recovery; and (4) pathogen loads decline quickly during recovery. We collected naturally infected bats at the end of hibernation, brought them into captivity, and quantified recovery over 40 days by monitoring body mass, wing damage, thermoregulation, histopathology of wing biopsies, skin surface lipids and fungal load. Most metrics returned to normal within 30 days, although wing damage was still detectable at the end of the study. Torpor expression declined overall throughout the study, but bats expressed relatively shallow torpor bouts – with a plateau in minimum skin temperature – during intensive healing between approximately days 8 and 15. Pathogen loads were nearly undetectable after the first week of the study, but some bats were still detectably infected at day 40. Our results suggest that healing bats face a severe energetic imbalance during early recovery from direct costs of healing and reduced foraging efficiency. Management of WNS should not rely solely on actions during winter, but should also aim to support energy balance of recovering bats during spring and summer.

KEY WORDS: Healing, Heterothermy, Histology, Lipid profiles, *Myotis lucifugus*, Wildlife disease

INTRODUCTION

Wildlife infectious diseases are increasing globally owing, in part, to human encroachment into natural habitats and increased travel and trade (Daszak et al., 2000; Jones et al., 2008). Dynamic population models are often used to describe the processes of infection and survival or recovery. In the classic SIR framework (susceptible, infected, recovered; Anderson and May, 1978), susceptible individuals in a population (S) become infected (I) and a subset of these survive disease pathology, after which they are considered recovered (R). In the context of so-called 'conservation pathogens' (Willis, 2015) which can cause high host mortality, understanding the transition from I to R is crucial because management actions that support the I–R transition may be among the most effective for conservation and recovery of host populations (Fenner, 2010), especially for hosts with long generation times (Vander Wal et al., 2013; Carlson et al., 2014). Recovery involves restoration of physiological and behavioral function, and healing of tissues damaged by disease. Therefore, recovery from severe disease often involves a pronounced period during which physiological, behavioral and reproductive performance are impaired by the direct effects of damaged tissue or indirect effects of reallocation of resources to recovery (Peckarsky et al., 1993; Sheriff et al., 2009; Bowerman et al., 2010).

Although hosts regenerate damaged tissue, restore homeostasis and clear infection during the transition from I to R (Smith, 1994), lingering infection can still negatively affect recovery through immune responses that counteract healing (e.g. tissue damage owing to inflammation; Meteyer et al., 2012). Recovery can also influence host–host transmission and infection dynamics. Individual pathogen load, and potential to shed pathogens, likely declines during recovery compared with earlier disease stages. However, in the case of some pathogens, clearing infection can increase shedding of the active pathogen to susceptible conspecifics or to an environmental reservoir (Langwig et al., 2015; Huebschman et al., 2019). Despite surviving disease, a recovering host may still spread a pathogen to naïve hosts or new populations. Therefore, quantifying pathogen loads during recovery is important for understanding links between recovery of individuals and their potential to transmit a pathogen throughout their population.

Fungal diseases of wildlife have received recent attention, as they appear to be increasing with climate change and economic globalization, and because they have caused catastrophic population declines in a range of taxa (Fisher et al., 2012). Fungal pathogens of vertebrates tend to target the skin and structures in the skin (e.g. hair follicles, glands), or glandular products of the skin (Meteyer et al., 2009; Rosenblum et al., 2010; Martel et al., 2013). These pathogens cause physiological disruption by permeating the skin, which can lead to mortality (Voyles et al., 2009; Cryan et al., 2010; Martel et al., 2013; Warnecke et al., 2013; Verant et al., 2014), but for hosts that do not suffer mortality, there are often latent challenges associated with skin damage, including structural changes to locomotor and sensory organs (Parris and Beaudoin, 2004; Reichard and Kunz, 2009; Venesky et al., 2009; Chatfield et al., 2013; Hanlon et al., 2015), which can influence survival and reproduction after primary pathology has subsided.

[1]Department of Biological Sciences, Texas Tech University, 2901 Main Street, Lubbock, TX 79409, USA. [2]Department of Oncology, Lombardi Comprehensive Cancer Center, Georgetown University Medical Center, 3970 Reservoir Road NW, Washington, DC 20057, USA. [3]Department of Biology, Boston University, 5 Cummington Mall, Boston, MA 02215, USA. [4]Department of Microbiology and Immunology, Montana State University, Bozeman, MT 59717, USA. [5]Department of Ecology and Evolutionary Biology, University of Toronto Mississauga, 3359 Mississauga Road, Mississauga, ON, Canada L5L 1C6. [6]Arkansas Biosciences Institute, Arkansas State University, P.O. Box 847, Jonesboro, AR 72467, USA. [7]Department of Biology and Centre for Forest Inter-Disciplinary Research (C-FIR), University of Winnipeg, 515 Portage Avenue, Winnipeg, MB, Canada R3B 2E9.

*Author for correspondence (nw.fuller@ttu.edu)

N.W.F., 0000-0003-2185-3646; E.L.P., 0000-0002-4953-9715

Received 5 August 2019; Accepted 10 February 2020

Journal of Experimental Biology (2020) 223, jeb211912. doi:10.1242/jeb.211912

List of symbols and abbreviations

GAMM	generalized additive mixed model
GC	gas chromatograph
HI	heterothermy index
MS	mass spectrometer
PC	principal component
PCA	principal component analysis
qPCR	quantitative PCR
SIR	susceptible – infected – recovered
T_a	ambient temperature
T_b	body temperature
T_{sk}	skin temperature
$T_{sk,min}$	daily minimum skin temperature
UV	ultraviolet
WNS	white-nose syndrome

White-nose syndrome (WNS) is a fungal disease, caused by *Pseudogymnoascus destructans*, that affects hibernating bats and provides an opportunity to understand the recovery phase of disease, as individuals transition from I to R in the SIR framework. WNS is thought to cause mortality through skin damage and physiological disruption (Cryan et al., 2010; Warnecke et al., 2013; Verant et al., 2014). Although WNS causes high mortality in many North American species, there is now evidence of survivors persisting years after initial population declines in some affected regions (Dobony et al., 2011; Reichard et al., 2014; Langwig et al., 2017). These individuals have persisted despite the pathophysiological consequences of *P. destructans* during winter hibernation, when most mortality occurs, and have also survived lingering impacts of the disease, including low body mass and severe wing damage (Reichard and Kunz, 2009), that occur after hibernation. Understanding the processes by which bats endure and recover from WNS may help in the development of disease mitigation strategies.

There are multiple consequences of wing damage for individuals with WNS. Damage to the epithelium and pilosebaceous units reduces total lipids on flight membranes (Pannkuk et al., 2015). Skin surface lipids protect and lubricate while providing antimicrobial benefits (Desbois and Smith, 2010), so these changes could impact wing condition and increase secondary infections during recovery. Structural changes to flight membranes, such as scabs, holes and loss of sensory hairs, may also reduce flight efficiency (Sterbing-D'Angelo et al., 2011; Voigt, 2013; Marshall et al., 2015). Impaired flight performance will reduce foraging success of recovering bats during a time when insect abundance is often low and ephemeral (Anthony and Kunz, 1977). This could, in turn, reduce fitness of WNS survivors because they must reallocate resources from reproduction to tissue healing and accumulation of fat stores. Recovering bats may also need to depend more heavily on torpor [i.e. reduced body temperature (T_b) and metabolic rate], which is known to slow fetal development and delay parturition (Racey and Swift, 1981; Racey, 1982). Given these effects, WNS provides an opportunity to study recovery from disease and the ecological effects of sublethal injury.

We conducted a longitudinal study of post-WNS recovery in little brown bats [*Myotis lucifugus* (Le Conte 1831)] naturally infected with *P. destructans*, to address three objectives: (1) determine the duration of the post-hibernation healing period and describe the healing process; (2) determine how skin structure and function are restored during healing; and (3) quantify prevalence and intensity of infection throughout healing. To address objective 1, we first tested whether body mass and wing damage would recover to a normal, healthy state at a rate consistent with free-ranging bats during spring (Fuller et al., 2011). Second, we tested whether torpor use plays a role in the healing process, especially during early healing, because this is the phase of recovery when bats are most likely to face negative energy balance. We predicted that bats would recover body mass and wing integrity within 30 days of removal from late hibernation and arrival at our captive facility and that torpor use would be greatest during the early phases of healing, when bats face the most pronounced energetic investment in tissue regeneration but have the lowest body mass and smallest energy reserves. To address objective 2, we quantified skin surface lipids as a proxy for wing physiological function and conducted histological analysis of healing wing tissue to test the hypothesis that wing surface lipids would recover on the same timescale as body mass and wing structure. We predicted that the skin surface lipid profile (relative proportions of different fatty acids) would change throughout healing, back to a lipid profile reflective of normal, healthy skin (Pannkuk et al., 2014). To address objective 3, we collected standardized swabs for qPCR analysis of pathogen load to test the hypothesis that the potential of bats to spread *P. destructans* declines as they heal and recover. We predicted that recovering bats would clear infection on a similar time scale as recovery from other aspects of disease pathology.

MATERIALS AND METHODS

Between 27 and 30 April 2013, we collected 16 male little brown bats from two sites near Ottawa, Canada. Sites were WNS-positive for 3–5 years at the time of collection (USFWS, 2019; https://www.whitenosesyndrome.org/static-page/wns-spread-maps). We visited sites at the end of hibernation to increase the likelihood that individuals we collected would have survived the disease in the wild. We removed torpid bats from walls/ceilings of hibernacula by hand and placed them into clean, individually numbered cloth holding bags. We recorded mass (±0.1 g), forearm length (±0.1 mm) and wing damage score following Reichard and Kunz (2009) for all bats at the time of capture. We also photographed both wings of each bat (see below). To confirm infection, we used standard protocols (e.g. Bernard et al., 2017) to collect swabs for qPCR analysis (see below). Each bat was fitted with a temperature datalogger (iButton, Maxim Integrated Products, San Jose, CA, USA) to record skin temperature (T_{sk}; ±0.5°C) every 15 min so we could quantify torpor use. Modified iButtons (Lovegrove, 2009; Reeder et al., 2012) were attached to the intrascapular region using ostomy cement (Ostobond, Montreal Ostomy, Montreal, Quebec, Canada). Bats were then transported to the University of Winnipeg in a temperature-controlled chamber (8°C) lined with wet towels to maintain high humidity, as described by Warnecke et al. (2012).

At the University of Winnipeg, bats were housed in a flight cage (2.24 m long×1 m wide×2.42 m high) inside a biosecure animal holding room maintained at an ambient temperature (T_a) of 18°C and 60% relative humidity with a light:dark cycle matching the natural photoperiod at the latitude of the capture site (11 h:13 h light:dark). The temperature (18°C) and humidity (60%) represent the minimum temperature and maximum humidity that could be maintained by the air handling system in the facility. When first brought into the facility, bats were hand fed mealworms, gut-loaded by housing them in a mix of wheat, powdered milk and nutrient supplements (calcium, minerals and vitamins) following Lollar and French (1998), Racey (1970), and advice from colleagues with expertise in bat husbandry (P. Faure, personal communication). This diet is high in calories and fat and provides essential nutrients (Lollar and French, 1998). Little is known about the natural diet of little brown bats during this time of year, but little brown bats are

Journal of Experimental Biology (2020) 223, jeb211912. doi:10.1242/jeb.211912

generalist predators and consume a wide variety of insect taxa. Mealworms are likely high in saturated fat, especially palmitic acid (16:0), relative to a natural diet (Jones et al., 1972; Dreassi et al., 2017), but we provided the nutritional supplement Nutri-cal (Tomlyn Veterinary Science, Fort Worth, TX, USA) to ensure bats obtained essential fatty acids and other nutrients during the initial 10 days of captivity, until they learned to self-feed. Once all bats were self-feeding, mealworms and water were provided *ad libitum* on a small table in the center of the flight cage. We could not perfectly replicate a natural diet but the mealworm medium plus nutritional supplements provided a variety of essential vitamins, minerals and fatty acids that reasonably approximate the diet available to wild animals.

Roosting space was provided by a three-chamber wooden bat box mounted on a pole 2.5 m above the floor and several large towels that were hung on the side of the cage. Little brown bats are difficult to maintain in captivity during the active season and, in the absence of data on their preferred roost temperatures during spring, we provided a range of roost temperatures to allow bats to choose a preferred temperature and reduce stress, and to better approximate the kind of environmental variation they might experience in the wild. Therefore, the back chamber of the roost box was equipped with a heating coil designed for reptile terraria (Exoterra Temperature Heating Cable, 12 V; Rolf C. Hagen Group, Mansfield, MA, USA) connected to a thermostat (Ranco Nema 4× Electircal Temperature Control; Invensys, Plain City, OH, USA) set to 30°C, slightly below the lower end of the thermoneutral zone for little brown bats (Stones and Wiebers, 1965, Speakman and Thomas, 2003; see Wilcox and Willis, 2016 for description of heated box). Thus, the box provided a range of temperatures from 18°C to 30°C. To our knowledge, there are no data available on temperatures of roosts selected by little brown bats immediately after emergence from hibernation. Although 30°C is likely warm relative to roosts used by free-ranging little brown bats in the wild, many roosts, especially those in the roofs of buildings, could provide temperatures this high owing to solar heat gain, while also providing a range of colder temperatures. Thus, while the roosting environment in our captive setting was artificial, it provided a range of temperatures approximating what bats might access in the wild. Some bats roosted inside the heated box daily and others often roosted on the mesh wall of the flight cage. No bats were found roosting in the towels. Before and after handling bats, all equipment was disinfected in a 1:16 solution of Accel® Disinfectant (Virox Technologies, Oakville, ON, Canada).

We monitored the healing process for 40 days from the date of capture, recording data or collecting samples to quantify body mass, wing damage, torpor expression, skin surface lipids, histopathology and the presence of fungus at intervals ranging from daily to once during a 2 week period (Fig. 1). To reduce stress, we only conducted lipid sampling, tissue collection for histopathology and swabbing for qPCR analysis five times throughout the study. Sampling that was less disruptive to the bats (i.e. body mass, wing photographs) was conducted more often (Fig. 1).

We recorded body mass (±0.1 g) twice daily during the first 12 days of captivity, between 09:00 and 12:00 h and 16:00 and 18:00 h, to identify individuals that required hand-feeding, and to identify distressed bats for humane euthanasia, based on rapidly declining body mass. All 16 bats were suffering from advanced WNS at the time of capture and five required euthanasia (via CO_2 exposure under isoflurane anesthesia) during the first 2 weeks of the study. However, after this initial period, the remaining bats gained body mass and survived to the completion of the study. Thus, for all variables in this study, except for torpor expression data (see below), our sample size was 11 animals.

We captured digital photographs to document changes in wing damage during the recovery process. We photographed bat wings transilluminated with white fluorescent light at 15 time points and with ultraviolet (UV) light at eight time points (Fig. 1) following techniques established by Reichard and Kunz (2009), modified by Fuller et al. (2011) for visible light wavelengths (approximately 390–700 nm) and by Turner et al. (2014) for long-wave UV light (366–385 nm). We documented four visually distinct categories of wing membrane deformation based on photo analysis (see Results). Damage that was apparent using white fluorescent illumination was categorized as either black lesions or white discoloration (Fig. S1A). Illumination with UV light revealed areas of orange and teal fluorescence (Fig. S1B). Black lesions and orange and teal fluorescence were typically present in discrete points, and thus were quantified based on the number of points, whereas white spots visible under fluorescent light were more globular and diffuse, so we quantified these based on total area. To determine the amount (mean number of lesions across both wings) and extent (total damaged area across both wings) of each type of wing damage, we used the region of interest selector and manager in ImageJ (v1.47; Schneider et al., 2012) following Fuller et al. (2011). Scale was provided by a Canadian $1 coin. Small areas of the wing were obscured by fingers of researchers holding the bats in some photos, so we only used damage to the plagiopatagium, which was always well illuminated and clearly visible, for statistical analysis (Fuller et al., 2011). All photographic analysis was conducted by one researcher (N.W.F.) for consistency.

We quantified torpor expression by calculating daily heterothermy index (a metric that combines depth and duration of torpor; Boyles et al., 2011, Boyles, 2019) and daily minimum T_{sk} ($T_{sk,min}$) for each bat with at least 20 days of T_{sk} data (n=7). We chose 20 days because by day 25 of the study some bats had shed

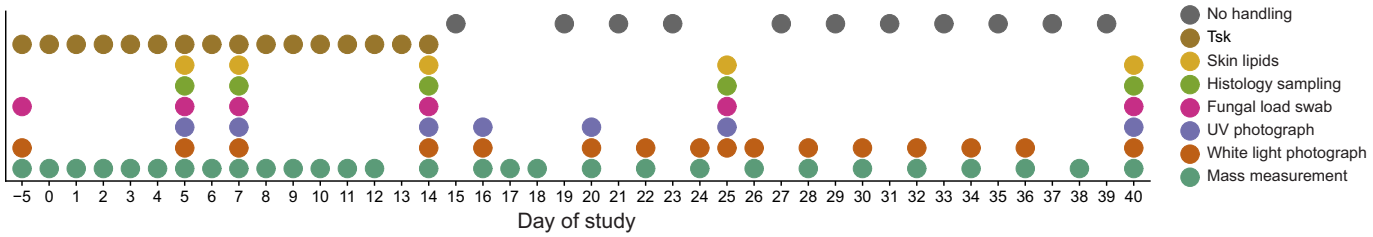

Fig. 1. Timeline of sampling events during this study. Colored dots indicate that a sample was collected during the corresponding day of the study. Day −5 to day 0 represents capture and transport to the University of Winnipeg. Mass was recorded twice daily (between 09:00 and 12:00 h and again between 16:00 and 18:00 h) during the first 12 days of the study as part of a monitoring strategy to provide care for recovering bats and to identify individuals that required humane euthanasia.

their temperature dataloggers. Filtering the data at day 20 ensured that we presented information from a time during which all bats experienced the same conditions. Daily heterothermy index (HI) was calculated following Boyles et al. (2011) for each bat on each day. Because HI is most useful in a comparative context, we used HI values as a measure of overall change in torpor expression per individual over time. To account for high body temperatures during handling, we excluded T_{sk} measurements from 09:00 to 12:00 h on each handling day, and 16:00 to 18:00 h during the first 12 days of the study when bats were handled twice daily, and the entire daylight period on days when we conducted invasive sampling (Fig. 1).

To measure skin function, we collected wing surface lipids following Pannkuk et al. (2014) from each individual at the same five time points as swabbing and histological sampling (Fig. 1). We selected a location on the plagiopatagium by targeting an area of UV fluorescence. We affixed a strip of SebuTape® (CuDerm Corporation, Dallas, TX, USA) to the wing for 1 min and then removed it with forceps. We placed the strip into a 4 ml vial with a Teflon® lined cap (Fisher Scientific, Pittsburgh, PA, USA) containing approximately 2 ml of 3:2 chloroform:methanol with 0.1% butylated hydroxytoluene (VWR International, Radnor, PA, USA) to prevent oxidation of lipids. The vials were held at −20°C for 12 h, after which we removed the SebuTape® strips and stored the samples at −20°C for up to 30 days. Samples were shipped on dry ice overnight to the Arkansas Biosciences Institute (Jonesboro, AR, USA), and stored at −20°C prior to analysis.

The collected surface lipids were esterified to fatty acid methyl esters (FAMEs) and quantified on a Varian (Santa Clara, CA, USA) 450-gas chromatograph (GC) unit equipped with an Agilent Durabond HP-88 column and a Varian CP-8400 autosampler coupled to an ion trap Varian 240-MS/4000 mass spectrometer (MS). Operating conditions for GC injector temperatures, transfer line temperatures, EI-MS, manifold, transfer-line and trap temperatures were performed as previously described (Pannkuk et al., 2013, 2014). Target peaks were identified by reference to an authentic standard and matching electron ionization spectra to the NIST/EPA/NIH Mass Spectral Library (NIST 11) and the NIST Mass Spectral Search Program (Version 2.0f, Gaithersburg, MD, USA). We excluded fatty acids that represented <1% of the total from analysis. Proportions of major fatty acids were arcsine-square root transformed for analysis.

We collected wing biopsies from each bat twice, once from each wing at an interval of 1 to 2 weeks apart (Fig. 1). The subset of bats sampled on each sampling day was determined randomly. We located bright areas of fluorescence to biopsy by transilluminating the wing with UV light. Later in the study, after fluorescence subsided, we targeted lesions that were visually distinct with white light transillumination. To prevent contraction of biopsied tissue, the dorsal side of the wing was lightly moistened with water using a cotton swab, which adhered the skin to a small nitrocellulose filter (0.22 µm pore size; Millipore Corporation, catalog no. GSWP 013 00). The tissue was then excised using a 6 mm biopsy punch (Tru-Punch™, Sklar Corp., West Chester, PA, USA), and held between two sponges inside a histology cassette. Biopsies were stored in 10% formalin for >48 h (up to 2 weeks) and embedded in paraffin. We aligned biopsies in embedding molds so that the resulting sections would be lateral transects of tissue and sectioned at 4 µm. We modified an established protocol for periodic acid–Schiff staining for *P. destructans* (Meteyer et al., 2009), using light green counterstain (Electron Microscopy Sciences, catalog no. 17920) to enhance contrast of fungal tissue.

We used a compound light microscope (40X magnification, Model CM E, Leica Microsystems, Buffalo, NY, USA) to quantify the extent of fungal growth, number of cupping erosions and proportion of the tissue with inflammatory crust on the skin surface. We quantified the extent of fungal growth by dividing the section into 10 equally sized parts and counting the number that contained fungal hyphae. We counted the number of cupping erosions and estimated the proportion of the section in which inflammatory crust was the major feature as described by Meteyer et al. (2009). Small sample sizes precluded statistical analyses of histology data, and our description of histology results is qualitative, because we were limited to one sample per wing from a few individuals.

We quantified fungal load via quantitative PCR (qPCR) by collecting swabs of the flight membranes at capture and at each of our five weekly time points (Fig. 1). We also swabbed favored roosting areas, such as inside the heated box and mesh walls of the flight cages, to determine whether roosting areas harbored fungus. We followed standard swabbing protocols (Bernard et al., 2017) and stored swabs in RNAlater at −20°C until they were shipped on dry ice to Northern Arizona University for qPCR analysis following Muller et al. (2013), using 40 cycles as a cut-off for a positive detection.

All statistical analyses were performed in R (v3.1.1; https://www.r-project.org/). We used generalized additive mixed models (GAMMs) to describe non-linear patterns and included individual as a random effect to account for repeated measures. In all cases, we included the day of the study on which the measurement was taken (hereafter 'day of measurement') as the smoothing term. All models followed the format $y=s$(day of measurement), with y as the variable of interest (e.g. mass, wing damage, pathogen load) and s(day of measurement) as a smoothing term for the non-linear relationships generated by the GAMM analysis. To determine differences between study days, we used pairwise Kruskal–Wallis tests, followed by a *post hoc* Dunn's test using Bonferroni correction to account for multiple pairwise comparisons. We compared all days with the initial measurement day for each variable. We used principal component analysis (PCA) to reduce the dimensionality of the surface lipid data. We used the arc-sin transformed relative proportions of fatty acids in the PCA and retained the first two principal components (PCs) for evaluation. We used GAMMs to plot the changes in PC1 and PC2 of the fatty acids over time, using the same smoothing term as above. Significance was assessed at 0.05 and values are reported as means±s.e.m. All procedures were conducted under Québec Ministère du Développement durable, de l'Environnement, de la Faune et des Parcs and Ontario Ministry of Natural Resources permits and approved by the University of Winnipeg Animal Care Committee.

RESULTS

Mean body mass at capture was 7.1±0.08 g and declined to 5.7±0.09 g during the 2 days of transport to the University of Winnipeg. However, individuals gained body mass (3.8±0.77 g) rapidly during the study and mass plateaued at 9.0±0.23 g by day 24 (Fig. 2). Day of measurement explained 72.6% of the variation in body mass (F=514.9, edf=2.87, P<0.001; Fig. 2). Body mass increased above initial body mass by day 12 of the study (H=233.2, d.f.=27, P_{adj}=0.028; Fig. 2). On day 17, a malfunction caused the lights to remain on overnight and bats lost 1.3±0.25 g on this night but quickly recovered once the system was repaired the following day (Fig. 2, red points).

Healing progressed rapidly, although temporal trends varied with the type of damage (Fig. 3A–E). Under visible light

Journal of Experimental Biology (2020) 223, jeb211912. doi:10.1242/jeb.211912

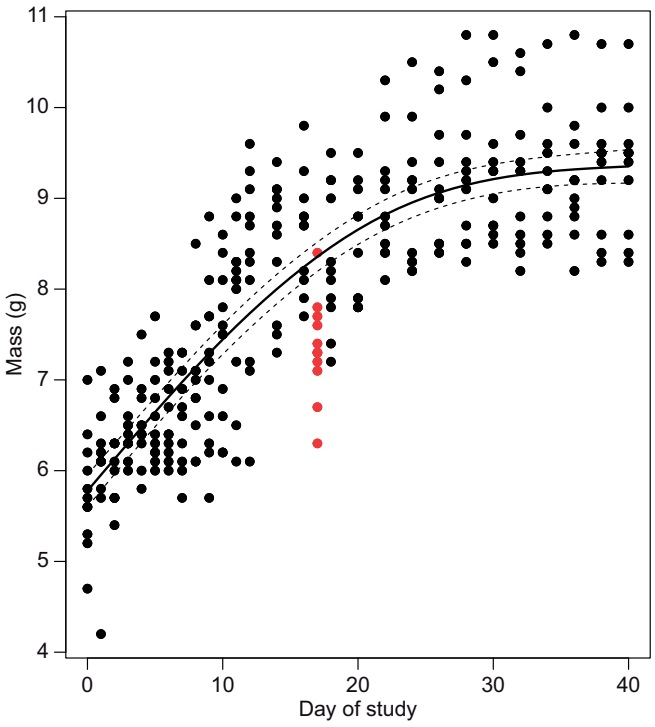

Fig. 2. Increasing body mass of little brown bats recovering from white-nose syndrome (WNS; *n*=11). Mean daily body mass is reported where body mass was recorded twice in one day (days 0–12). The red points show a brief decline in mass owing to a lighting malfunction on day 17, after which bats regained mass rapidly. Mean body mass was greater than arrival mass by day 12. The solid line indicates the GAMM model fit, and dashed lines indicate ±2 s.e.

transillumination we observed two different types of wing damage. Early in the healing process wing damage was characterized by black lesions (Fig. 3B,C), while later in the healing process (Fig. 3D) damaged wings were predominantly characterized by white coloration (Fig. 4A,B). Day of measurement explained 64.2% of the observed variation in black lesions (F=76.1, edf=2.96, P<0.001), and 30.9% of the variation in white discoloration (F=17.4, edf=2.89, P<0.001). Black lesions increased to peak abundance by day 14 (mean lesion count: 391.4±50.2). After this peak, mean lesion count declined by day 25 (mean lesion count: 207.2±28.6) and each day thereafter (H=85.5, d.f.=10, P_{adj}=0.022). White discoloration was minimal at the beginning of recovery (mean discolored area: 0.17±0.09 cm^2) and was not present in high abundance until after peak abundance of black lesions (day 30, mean discolored area: 3.80±0.97 cm^2). Areas of white damage were often preceded by black lesions (Fig. 3C,D).

Under UV transillumination, we observed two different types of wing damage. Lesions characterized by orange and teal fluorescence were both most abundant on the first day of measurement (day 5, mean orange lesion count: 63.2±12.2; mean teal lesion count: 22.6±6.3; Fig. 3A) and declined throughout healing (Fig. 4C,D). Day of measurement explained 55.7% of the variation in orange lesion count (F=52.0, edf=2.86, P<0.001). Orange lesion count declined below initial values by day 20 (mean lesion count: 2.9±1.8; H=58.89, d.f.=7, P_{adj}>0.001), and remained low. Teal lesions decreased from initial count by day 20 (mean lesion count: 2.4±1.2; H=48.0, d.f.=7, P_{adj}=0.022), and remained low. Time of measurement explained 36.7% of the variation in teal lesions (F=30.5, edf=2.39, P<0.001). Unlike black and white damage, where black lesions appeared to give way to white discoloration, there was no apparent association between orange and teal lesions.

Torpor expression, based on the HI, declined over time (R^2_{adj}=0.156, F=27.7, edf=1, P<0.001) and daily $T_{sk,min}$ increased with time (R^2_{adj}=0.126, F=23.87, edf=1, P<0.001), with a clear plateau in $T_{sk,min}$ during a period of rapid healing between days 8 and 15 (Fig. 5C). Bats with lower body mass used torpor more often (R^2_{adj}=0.273, F=26.9, edf=2.46, P<0.001) and used deeper torpor than larger bats (R^2_{adj}=0.147, F=36.4, edf=1.02, P<0.001), but there was no direct relationship between wing damage score and torpor expression (R^2_{adj}=0.05, F=2.1, edf=1.92, P>0.05).

The most common skin surface free fatty acids were palmitic (16:0), stearic (18:0), oleic (18:1n9) and linoleic acid (18:2n6), which were present in varying proportions over time. The first two components of a PCA explained 82% of the total variance in lipid changes (61% and 21%, respectively) (Table S1, Fig. 6). The first principal component (PC1) reflected saturation (saturated and unsaturated fatty acids) while the second component (PC2) reflected chain length. Unsaturated fatty acids [e.g. oleic, linoleic, α-linoleic (18:3n3) and gondoic (20:1n9) acids] were common early but declined within 30 days (R^2_{adj}=0.734, F=73.7, edf=2.85, P<0.001) while the proportion of saturated fatty acids (e.g. palmitic and stearic acids) increased (R^2_{adj}=0.529, F=26.0, edf=2.79, P<0.001; Fig. 6A). Concurrent with a shift from unsaturated to saturated fatty acids, fatty acid chain length varied, with long-chain fatty acids (18 carbon chain) dominant early and late in recovery and a peak period where very long-chain (>20 carbon chain) fatty acids were dominant (Fig. 6B).

Histopathological examination revealed dramatic and rapid changes in tissue structure and the presence of fungus. Initially, fungal hyphae were abundant in all individuals (Fig. S2A), and gradually decreased over time, with some bats clear of visible fungus by day 25 and only one bat retaining fungus to day 40. Fungus was mainly present in diffuse patches on the epidermis (Fig. S2A,B). Later samples (e.g. days 25 and 40) showed small fungal foci that were not interconnected and sometimes included only a single hyphal fragment (Fig. S2C,D). Cupping erosions were not common in the samples we analyzed. No more than one cupping erosion was observed in a given sample (likely owing to our sampling protocol, which targeted single points of fluorescence), and no erosions were observed beyond day 14. Inflammatory crust was present on all but one individual until day 40. Crusts were less prevalent on days 5 and 7 compared with subsequent days. Crusts were often associated with, or found to encase, large foci of hyphae. Wing perforations resulted from areas where hyphal aggregations had formed erosions in the membrane but were also rare and did not arise until after day 25. Opposite sides of the perforation showed evidence of rapid cell proliferation and hyperkeratosis. We saw no evidence for specificity in fungal invasion; skin structures such as glandular features and hair follicles did not appear to be particularly susceptible to the fungus. Presence of fungal hyphae closely matched results from qPCR of wing swabs (see below).

Fungal growth was not extensive and not immediately apparent on all bats at the time of capture but, upon close inspection, all individuals had visual signs of WNS at capture and all swabs taken at capture tested positive for *P. destructans* (mean fungal load: 7.0×10^{-4}±2.0×10^{-4} ng). Fungal load decreased rapidly (R^2_{adj}=0.412, F=18.6, edf=2.86, P<0.001; Fig. 7) and, by day 7, load was lower than at capture (mean fungal load: 2.5×10^{-5}±6.21×10^{-6} ng; H=41.8, d.f.=5, P_{adj}=0.002). By day 14, load was near the limit of detection.

Journal of Experimental Biology (2020) 223, jeb211912. doi:10.1242/jeb.211912

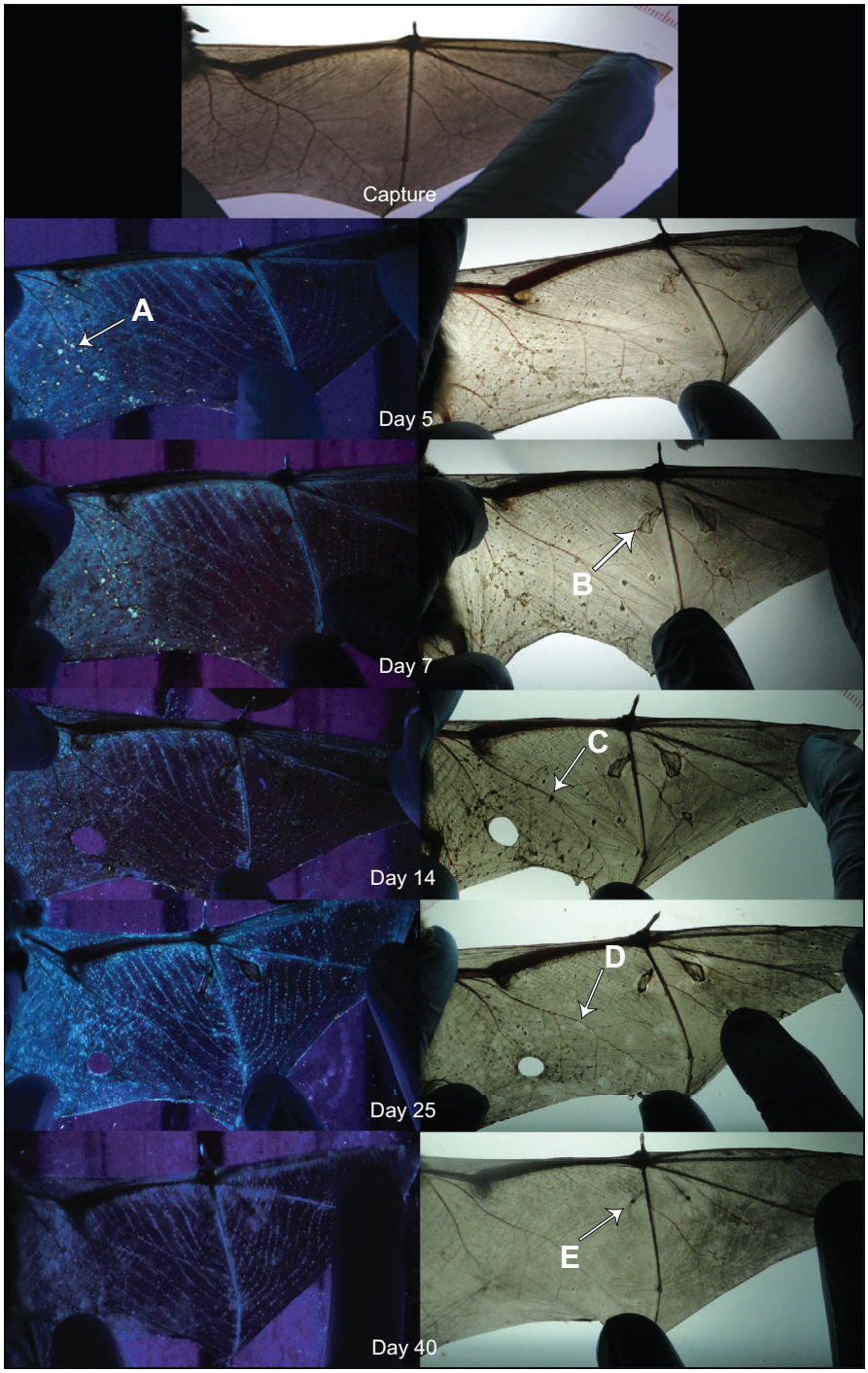

Fig. 3. The progression of wing damage recovery in survivors of WNS. At capture, wings appear normal when viewed with white light. Within 5 days, widespread fluorescence and lesions form on the wing (A). Lesions include large areas of crusts and scabs (B,C) that then develop into white discoloration (D). By day 40 of recovery, wings are almost fully healed, including contraction of large holes formed from deep erosions (E). The large hole that appears on day 14 is the result of sampling for histopathology and not related to damage caused by WNS.

Although histopathology only indicated fungus on one bat by day 40, qPCR identified four bats that remained *P. destructans*-positive throughout. An additional three individuals cleared infection and did not reacquire infection, while the remaining four individuals cleared infection but became infected again, albeit at very low levels.

DISCUSSION

Consistent with our predictions based on field data (Fuller et al., 2011), captive bats in our study recovered to a normal state quickly after hibernation, and most signs of disease, except wing damage, were gone within 2 weeks. Skin structure and body condition recovered over a time scale after hibernation consistent with other studies of healing from WNS or other injuries in free-ranging and captive bats (Faure et al., 2009; Weaver et al., 2009; Fuller et al., 2011; Meteyer et al., 2011; Ceballos-Vasquez et al., 2015; Pollock et al., 2015; Greville et al., 2018; Khayat et al., 2019; Davis and Doster, 1972). Following pathogen clearance, tissue damage caused by both the pathogen and inflammatory reactions (Meteyer et al., 2011, 2012) started to heal, and within 30 days of the start of our study, tissue damage was almost undetectable. Large holes and formerly widespread necrotic spots healed, intensity of infection subsided, and wing tissue resembled healthy skin both macroscopically and microscopically (Fig. 3E, and Fig. S2).

Journal of Experimental Biology (2020) 223, jeb211912. doi:10.1242/jeb.211912

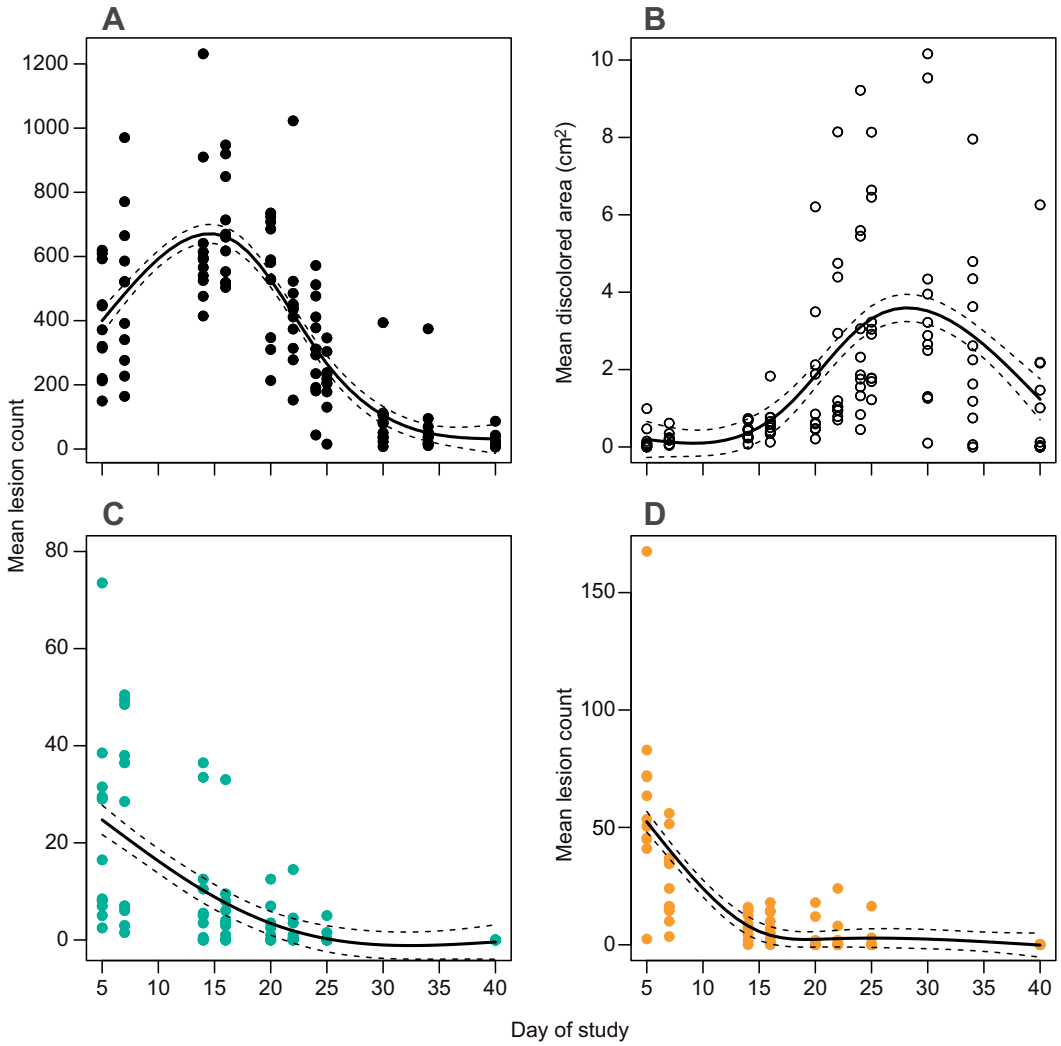

Fig. 4. Wing damage in little brown bats recovering from WNS (*n*=11). Solid lines indicate smoothing curves based on GAMM and dashed lines represent ±2 s.e. (A) Black lesion count increased to a peak on day 14, and then declined thereafter. (B) There was no white discoloration apparent at capture. Discoloration increased on day 14 and peaked on day 26. (C) Teal lesion count was high initially and declined continuously. (D) Orange lesion count followed a similar pattern to orange lesions.

Variation in torpor expression and body condition appeared to play a role in the healing process, suggesting that survivors of WNS face a challenge for energetic optimization during recovery. Despite *ad libitum* food and a range of roost temperatures, we observed regular torpor use and often found bats roosting outside the box where T_a would have facilitated torpor. Early in the healing process, bats regularly reduced T_{sk} to T_a (18°C), using the deepest torpor possible in our facility, presumably to maximize energy savings. Torpor expression was greatest early during recovery, when bats had the lowest body mass and most wing damage and torpor use declined over time. However, during the period of most rapid tissue restructuring (~days 8 to 15) there was a clear plateau in $T_{sk,min}$ (Fig. 5C) during which bats defended relatively high T_{sk} as much as 5–10°C above T_a. Flexible use of torpor could represent a trade-off between energy savings and immune function (Bouma et al., 2010). Reduced torpor expression could also reflect a fever response similar to that observed by Mayberry et al. (2018) for hibernating bats with WNS during arousals, and we recommend that future studies test this hypothesis by assessing expression of fever-mediating cytokines during WNS recovery (Evans et al., 2015; Lilley et al., 2017). WNS survivors must trade off investment in energetically costly healing against the need to maintain energy balance and, for females, investment in reproduction. For free-ranging bats, energetic costs of healing will likely be exacerbated by environmental conditions because, even without WNS, bats emerge from hibernation at a time when food availability is variable and T_a is still cold (Norquay et al., 2013). This suggests that torpor may play an even more important role in allowing free-ranging bats with WNS to budget energy in spring.

We were not able to detect a link between wing damage and torpor expression statistically. However, given the importance of metabolic processes for healing, and the downregulation of these processes during torpor (Prendergast et al., 2002; Bouma et al., 2010), we expect that such a connection exists in the wild. Our study determined damage by measuring scabbed lesions that appear after the post-hibernation peak inflammatory response to *P. destructans* and wing fluorescence. These lesions provide a good measure of overall wing damage but are not a direct index of the inflammatory response, which is thought to cause wing damage (Meteyer et al., 2012). In addition, variability in temporal patterns of torpor expression and healing make it difficult to detect an explicit link with a limited sample size. We recommend that future studies aim to

Journal of Experimental Biology (2020) 223, jeb211912. doi:10.1242/jeb.211912

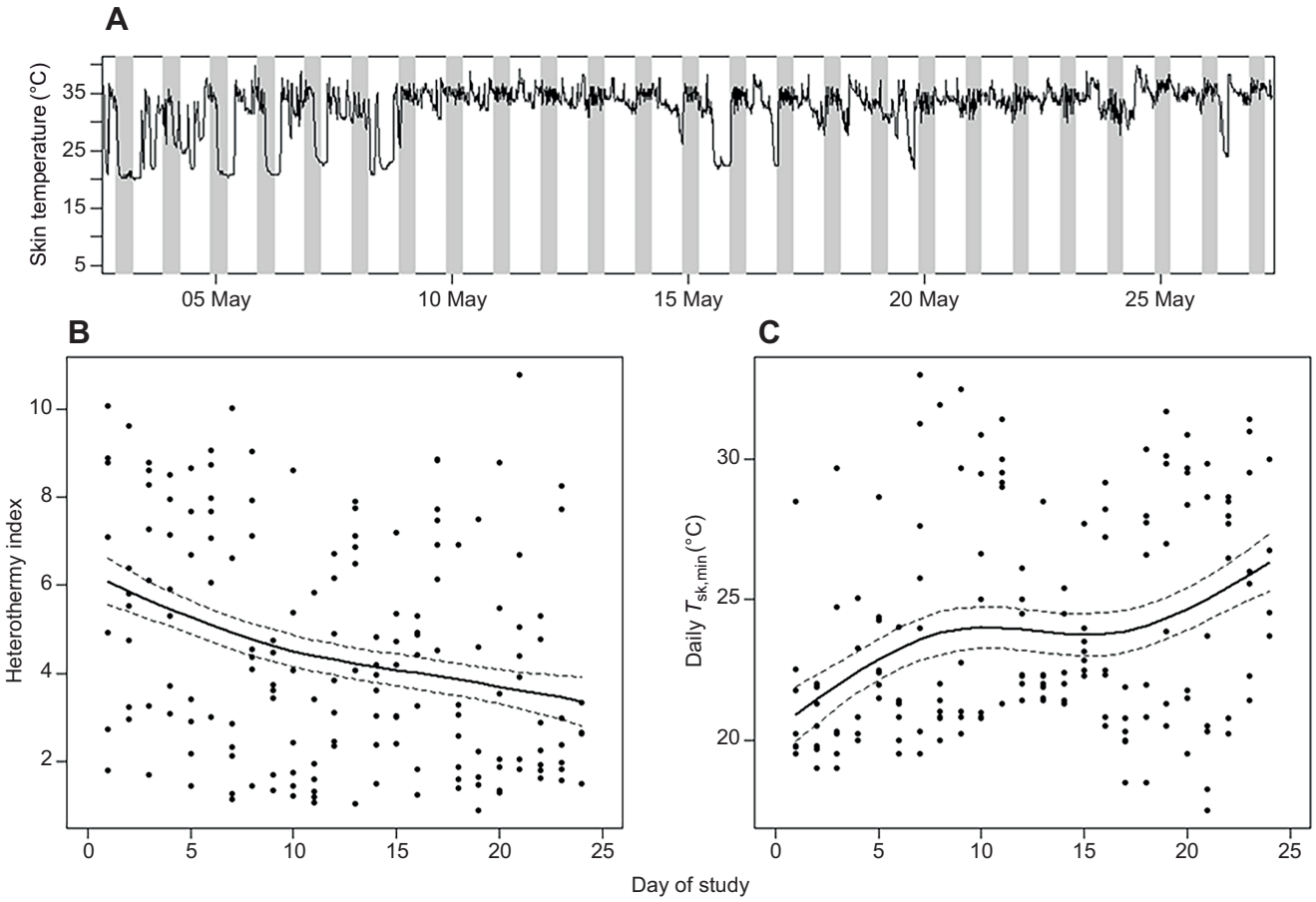

Fig. 5. Torpor expression in survivors of WNS. (A) Representative skin temperature (T_{sk}) traces for one bat from this study. Note the transition from regular daily torpor from 3 to 9 May to a long period of shallow torpor bouts from 9 to 15 May. Torpor expression (B) and torpor depth (C) are related to sampling date, concurrent with rapid increase in body mass (n=7). Solid lines indicate smoothing curves based on GAMM and dashed lines represent ±2 s.e.

directly connect inflammatory responses of individuals with variation in patterns of torpor expression for a larger sample of WNS survivors.

Skin surface lipids, our proxy for skin function, changed in saturation and chain length during and following peak wing damage. Lipid profiles returned to normal, pre-WNS levels (Pannkuk et al., 2014) on a similar time scale as body mass and wing condition, which suggests that glandular function was restored with healing alongside wing integrity. Although the function of wing surface lipids and glandular secretions from the wings of bats are not well understood, in general, skin surface lipids in mammals appear to serve a range of functions from helping reduce cutaneous water loss to preventing infection with bacterial pathogens (Ziboh et al., 2000; Feingold, 2007; Drake et al., 2008; Desbois and Smith, 2010). Thus, in addition to an energetic challenge during healing from WNS, bats may also face challenges associated with reduced skin function, increased water loss and increased risk of secondary skin infections. The torpor patterns we observed could counteract these challenges, because torpid animals experience reduced water loss and growth rates of pathogenic bacteria (Geiser and Brigham, 2012). Importantly, our results suggest that if bats can survive the initial challenging period after emergence skin function can recover quickly alongside skin structure.

Fungal load also declined as bats recovered from WNS. Within 10 days, *P. destructans* was only present at levels near the limit of detection, and some individuals had cleared the infection entirely. However, despite this encouraging decline in infection and the corresponding risk of transmission, some individuals reacquired *P. destructans* after most of the colony had cleared infection, suggesting that bats were still capable of infecting roostmates, or that the roost served as an environmental reservoir. Importantly, we only tested for *P. destructans* DNA and not viability of shed fungus.

Although the patterns observed in this study are consistent with studies of healing in free-ranging bats, our results may not fully reflect how bats recover in the wild. The bats in our study were in very poor condition at the start of the study because they were randomly sampled at the end of hibernation, before males had left the hibernaculum. Some individuals we captured may never have survived on their own, and their poor condition could have been exacerbated by long-distance transport. Bats in our study had ideal housing conditions, which may have accelerated healing relative to natural conditions. Finally, diet consisted of mealworms and nutrient supplements (Barnard, 2009), which may not fully replicate a natural diet (particularly relevant for lipid analysis; Pappas, 2009). However, because bats were provided a diet and supplements with a spectrum of nutrients, we expect that their diet was as close to natural as possible and that dietary essential fatty acids would facilitate synthesis of secreted lipids. Despite these differences, recovery occurred on a similar time scale as for free-ranging bats in the wild and, in our view, these results are useful for understanding the recovery process from WNS.

Journal of Experimental Biology (2020) 223, jeb211912. doi:10.1242/jeb.211912

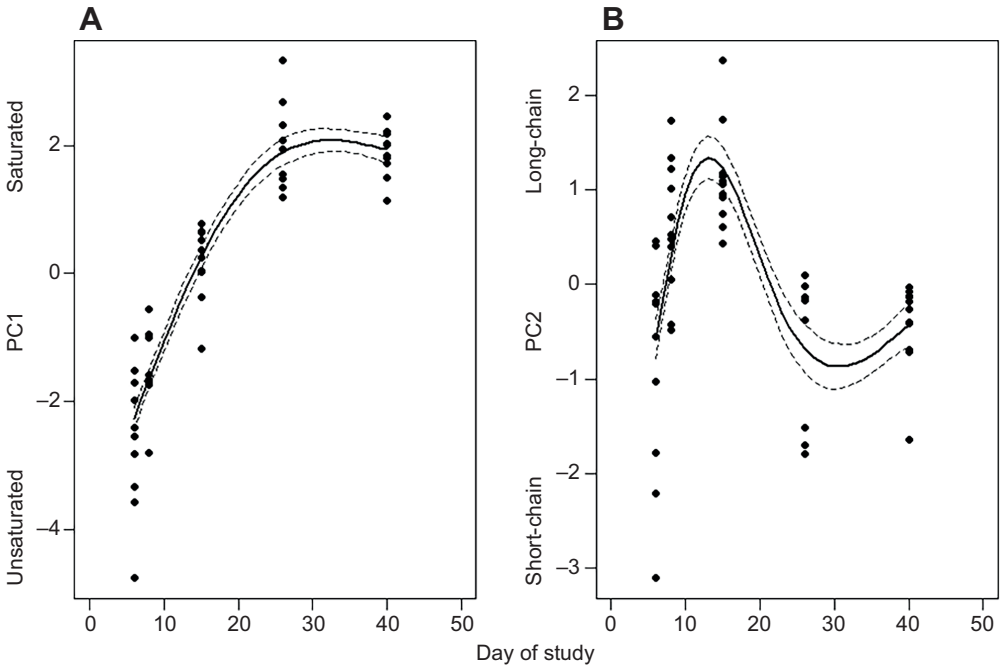

Fig. 6. The first two principal components of skin surface lipid patterns from little brown bats recovering from WNS (*n*=11) plotted over time. PC1 indicates a shift from unsaturated to saturated fatty acids (A), and PC2 indicates an increase in chain length (B) over time. Solid lines indicate smoothing curves based on GAMM and dashed lines represent ±2 s.e.

WNS is usually considered a disease of hibernation but our study highlights that population viability will depend not just on energetics of hibernation (Frank et al., 2019), but also energy balance during healing. Although there are few examples of wildlife disease as a driver of seasonal carryover effects, carryover (Norris, 2005; O'Connor et al., 2014) is thought to play a role in the impacts of WNS (Davy et al., 2017). There may be carryover effects from hibernation into the post-hibernation healing phase, and from the healing phase into reproduction (Davy et al., 2017). Torpor slows gestation and delays parturition (Racey and Swift, 1981; Dzal and Brigham, 2013), which may reduce the probability of pup survival beyond their first year (Frick et al., 2010). Alternatively, if reduced torpor expression is critical for healing and recovery, this could also negatively affect reproduction by increasing daily energetic demands and allocation of energy to recovery and thermoregulation rather than reproduction. It is important to note that our study was conducted with male bats. Female bats have different energetic requirements in spring and may select warm roosts, use shallower torpor or avoid torpor more often than males because of reproductive requirements (Hamilton and Barclay, 1994; Grinevitch et al., 1995; Dzal and Brigham, 2013). Although based on males, our results illustrate the additional energetic cost of WNS, which could have implications for reproduction by females. We recommend that future studies of WNS impacts and possible management actions quantify not just population size but rates of reproduction to assess the potential of carryover effects.

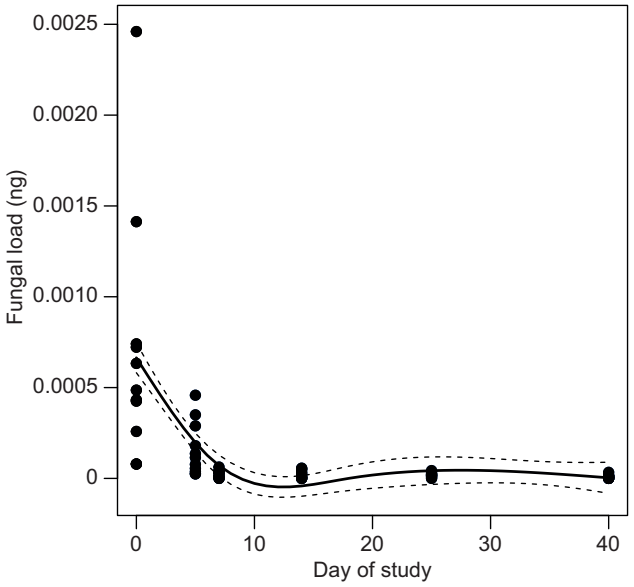

Fig. 7. Fungal load of *Pseudogymnoascus destructans* on little brown bats recovering from WNS (*n*=11). All bats tested positive for *P. destructans* at capture, fungal load decreased from initial values for the first 10 days of this study, and although values were very low by the conclusion of the study, infection persisted at low levels. Only one bat had detectable *P. destructans* by day 40. Solid lines indicate smoothing curves based on GAMM and dashed lines represent ±2 s.e.

The temporal pattern of torpor expression we observed during healing suggests that bats recovering from WNS may benefit from diverse roosting habitat. Bats expressed deep torpor most often during early healing, but $T_{sk,min}$ plateaued during the peak healing phase, which suggests they would benefit from roosts that are relatively cool much of the time, but that also receive solar exposure, allowing for passive rewarming (Geiser and Drury, 2003; Warnecke et al., 2008). This is similar to the changes in thermal requirements during the reproductive season, where male and non-reproductive female bats use deep torpor more often and roost away from maternity sites. Within maternity sites, bats select relatively warmer or cooler roosting locations based on their energetic requirements, whereas alternative non-maternity roosts (usually trees) are more suitable roosting habitat for deep torpor used by males and non-reproductive females (Hamilton and Barclay, 1994). Protecting or enhancing forest roosting habitat and/or providing artificial roosts that promote a range of roosting opportunities could be beneficial for WNS survivors. For example, Willis and Brigham (2007) found that cavity-roosting bats gain an energetic benefit from roost sharing with other individuals. Past forestry practices in North America have limited the number of large trees with cavities, forcing bats to use buildings as roosts. Forest management for mixed forest composition, including large trees with

cavities and snags, will provide varied roosting habitat for bats to choose based on energetic needs.

Effects of WNS clearly carry over to the active season, with potential implications both for spring survival and summer reproduction. Many conservation and management strategies currently being tested or planned focus primarily on actions to improve survival during hibernation. Our study suggests that management actions focused on helping bats achieve energy balance during post-hibernation WNS recovery could also be crucial for conservation of WNS-affected species.

Acknowledgements

We are extremely grateful to those who helped care for the captive colony: S. Bohn, Z. Czenze, A. Menzies, K. Muise, K. Norquay and A. Wilcox. D. Nickel and L. Buchanan provided space, solvents and assistance with histology preparations. J. Perry constructed bat roosts. Ontario Ministry of Natural Resources provided assistance in planning field work in Ontario. Anouk Simard (Québec Ministère des Ressources Naturelles et Faune), and Daniel Toussaint (Ministère du Développement durable, de l'Environnement, de la Faune et des Parcs) aided in planning and conducting field work in Québec. R. Bernard provided helpful feedback on an early version of the manuscript. J. Boyles provided neutral feedback on an early version of the manuscript.

Competing interests

The authors declare no competing or financial interests.

Author contributions

Conceptualization: N.W.F., L.P.M., C.K.R.W.; Methodology: N.W.F., L.P.M., E.L.P., T.B., C.K.R.W.; Formal analysis: N.W.F., L.P.M.; Investigation: N.W.F., L.P.M., E.L.P., T.B., H.W.M., C.K.R.W.; Resources: N.W.F., C.K.R.W.; Data curation: N.W.F., L.P.M., E.L.P., C.G.H.; Writing - original draft: N.W.F., L.P.M.; Writing - review & editing: N.W.F., L.P.M., E.L.P., T.B., C.G.H., H.W.M., C.K.R.W.; Visualization: N.W.F., L.P.M., C.G.H.; Supervision: L.P.M., T.S.R., C.K.R.W.; Project administration: H.W.M., C.K.R.W.; Funding acquisition: N.W.F., L.P.M., T.S.R., C.K.R.W.

Funding

This project was supported by a Bat Conservation International grant to N.W.F. and by grants from the United States Fish and Wildlife Service and Natural Sciences and Engineering Research Council of Canada (NSERC Discovery Grant) to C.K.R.W. L.P.M. was supported by a NSERC postdoctoral fellowship. E.L.P. was funded by the Arkansas State University Graduate Program in Environmental Sciences, a State Wildlife Grant from the Arkansas Game and Fish Commission to T.S.R., and the National Science Foundation (GC-MS instrumentation awarded to J. Bouldin, NSF 1040466). This project has been funded in whole or in part with Federal funds from the U.S. Department of Defense Strategic Environmental Research and Development Program, under Contract Number W912HQ-16-C-0015. Any opinions, findings, and conclusions or recommendations expressed in this publication are those of the author(s) and do not necessarily reflect the views of the Government.

Supplementary information

Supplementary information available online at
http://jeb.biologists.org/lookup/doi/10.1242/211912.supplemental

References

Anderson, R. M. and May, R. M. (1978). Regulation and stability of host-parasite population interactions: I. Regulatory processes. *J. Anim. Ecol.* **47**, 219-247. doi:10.2307/3933

Anthony, E. L. P. and Kunz, T. H. (1977). Feeding strategies of the little brown bat, *Myotis lucifugus*, in southern New Hampshire. *Ecology* **58**, 775-786. doi:10.2307/1936213

Barnard, S. M. (2009). *Bats in Captivity*. Logos Press.

Bernard, R. F., Willcox, E. V., Parise, K. L., Foster, J. T. and McCracken, G. F. (2017). White-nose syndrome fungus, *Pseudogymnoascus destructans*, on bats captured emerging from caves during winter in the southeastern United States. *BMC Zool.* **2**, 12. doi:10.1186/s40850-017-0021-2

Bouma, H. J., Carey, H. V. and Kroese, G. M. (2010). Hibernation: the immune system at rest? *J. Leukocyte Biol.* **88**, 619-624. doi:10.1189/jlb.0310174

Bowerman, J., Johnson, P. T. and Bowerman, T. (2010). Sublethal predators and their injured prey: linking aquatic predators and severe limb abnormalities in amphibians. *Ecology* **91**, 242-251. doi:10.1890/08-1687.1

Boyles, J. G. (2019). A brief introduction to methods for describing body temperature in endotherms. *Physiol. Biochem. Zool.* **92**, 365-372. doi:10.1086/703420

Boyles, J. G., Smit, B. and McKechnie, A. E. (2011). A new comparative metric for estimating heterothermy in endotherms. *Physiol. Biochem. Zool.* **84**, 115-123. doi:10.1086/656724

Carlson, S. M., Cunningham, C. J. and Westley, P. A. (2014). Evolutionary rescue in a changing world. *Trends Ecol. Evol.* **29**, 521-530. doi:10.1016/j.tree.2014.06.005

Ceballos-Vasquez, A., Caldwell, J. R. and Faure, P. A. (2015). Seasonal and reproductive effects on wound healing in the flight membranes of captive big brown bats. *Biol. Open* **4**, 95-103. doi:10.1242/bio.201410264

Chatfield, M. W. H., Brannelly, L. A., Robak, M. J., Freeborn, L., Lailvaux, S. P. and Richards-Zawacki, C. L. (2013). Fitness consequences of infection by *Batrachochytrium dendrobatidis* in northern leopard frogs (*Lithobates pipiens*). *Ecohealth* **10**, 90-98. doi:10.1007/s10393-013-0833-7

Cryan, P., Meteyer, C., Boyles, J. and Blehert, D. (2010). Wing pathology of white-nose syndrome in bats suggests life-threatening disruption of physiology. *BMC Biol.* **8**, 135. doi:10.1186/1741-7007-8-135

Daszak, P., Cunningham, A. A. and Hyatt, A. D. (2000). Emerging infectious diseases of wildlife: threats to biodiversity and human health. *Science* **287**, 443-449. doi:10.1126/science.287.5452.443

Davis, R. and Doster, S. E. (1972). Wing repair in pallid bats. *J. Mammal.* **53**, 377-378. doi:10.2307/1379180

Davy, C. M., Mastromonaco, G. F., Riley, J. L., Baxter-Gilbert, J. H., Mayberry, H. and Willis, C. K. R. (2017). Conservation implications of physiological carry-over effects in bats recovering from white-nose syndrome. *Conserv. Biol.* **31**, 615-624. doi:10.1111/cobi.12841

Desbois, A. P. and Smith, V. J. (2010). Antibacterial free fatty acids: activities, mechanisms of action and biotechnological potential. *Appl. Microbiol. Biotechnol.* **85**, 1629-1642. doi:10.1007/s00253-009-2355-3

Dobony, C. A., Hicks, A. C., Langwig, K. E., von Linden, R. I., Okoniewski, J. C. and Rainbolt, R. E. (2011). Little brown myotis persist despite exposure to white-nose syndrome. *J. Fish Wildl. Manag.* **2**, 190-195. doi:10.3996/022011-JFWM-014

Drake, D. R., Brogden, K. A., Dawson, D. V. and Wertz, P. W. (2008). Thematic review series: skin lipids. Antimicrobial lipids at the skin surface. *J. Lipid Res.* **49**, 4-11. doi:10.1194/jlr.R700016-JLR200

Dreassi, E., Cito, A., Zanfini, A., Materozzi, L., Botta, M. and Francardi, V. (2017). Dietary fatty acids influence the growth and fatty acid composition of the yellow mealworm *Tenebrio molitor* (Coleoptera: Tenebrionidae). *Lipids* **52**, 285-294. doi:10.1007/s11745-016-4220-3

Dzal, Y. A. and Brigham, R. M. (2013). The tradeoff between torpor use and reproduction in little brown bats (*Myotis lucifugus*). *J. Comp. Physiol. B* **183**, 279-288. doi:10.1007/s00360-012-0705-4

Evans, S. S., Repasky, E. A. and Fisher, D. T. (2015). Fever and the thermal regulation of immunity: the immune system feels the heat. *Nat. Rev. Immunol.* **15**, 335. doi:10.1038/nri3843

Faure, P. A., Re, D. E. and Clare, E. L. (2009). Wound healing in the flight membranes of big brown bats. *J. Mammal.* **90**, 1148-1156. doi:10.1644/08-MAMM-A-332.1

Feingold, K. R. (2007). Thematic review series: skin lipids. The role of epidermal lipids in cutaneous permeability barrier homeostasis. *J. Lipid Res.* **48**, 2531-2546. doi:10.1194/jlr.R700013-JLR200

Fenner, F. (2010). Deliberate introduction of the European rabbit, *Oryctolagus cuniculus*, into Australia. *Rev. Sci. Tech.* **29**, 103. doi:10.20506/rst.29.1.1964

Fisher, M. C., Henk, D. A., Briggs, C. J., Brownstein, J. S., Madoff, L. C., McCraw, S. L. and Gurr, S. J. (2012). Emerging fungal threats to animal, plant and ecosystem health. *Nature* **484**, 186-194. doi:10.1038/nature10947

Frank, C. L., Davis, A. D. and Herzog, C. (2019). The evolution of a bat population with white-nose syndrome (WNS) reveals a shift from an epizootic to an enzootic phase. *Front. Zool.* **16**, 1-9. doi:10.1186/s12983-019-0340-y

Frick, W. F., Reynolds, D. S. and Kunz, T. H. (2010). Influence of climate and reproductive timing on demography of little brown myotis *Myotis lucifugus*. *J. Anim. Ecol.* **79**, 128-136. doi:10.1111/j.1365-2656.2009.01615.x

Fuller, N. W., Reichard, J. D., Nabhan, M. L., Fellows, S. R., Pepin, L. C. and Kunz, T. H. (2011). Free-ranging little brown myotis (*Myotis lucifugus*) heal from wing damage associated with white-nose syndrome. *Ecohealth* **8**, 154-162. doi:10.1007/s10393-011-0705-y

Geiser, F. and Drury, R. (2003). Radiant heat affects thermoregulation and energy expenditure during rewarming from torpor. *J. Comp. Physiol. B* **173**, 55-60. doi:10.1007/s00360-002-0311-y

Geiser, F. and Brigham, R. M. (2012). The other functions of torpor. In *Living in a Seasonal World: Thermoregulatory and Metabolic Adaptations* (ed. T. Ruf, C. Bieber, W. Arnold and E. Millesi), pp. 109-121. Berlin, Heidelberg: Springer.

Greville, L. J., Ceballos-Vasquez, A., Valdizón-Rodríguez, R., Caldwell, J. R. and Faure, P. A. (2018). Wound healing in wing membranes of the Egyptian fruit bat (*Rousettus aegyptiacus*) and big brown bat (*Eptesicus fuscus*). *J. Mammal.* **99**, 974-982. doi:10.1093/jmammal/gyy050

Grinevitch, L., Holroyd, S. L. and Barclay, R. M. R. (1995). Sex differences in the use of daily torpor and foraging time by big brown bats (*Eptesicus fuscus*) during

the reproductive season. *J. Zool.* **235**, 301-309. doi:10.1111/j.1469-7998.1995.tb05146.x
Hamilton, I. M. and Barclay, R. M. (1994). Patterns of daily torpor and day-roost selection by male and female big brown bats (*Eptesicus fuscus*). *Can. J. Zool.* **72**, 744-749. doi:10.1139/z94-100
Hanlon, S. M., Lynch, K. J., Kerby, J. and Parris, M. J. (2015). Batrachochytrium dendrobatidis exposure effects on foraging efficiencies and body size in anuran tadpoles. *Dis. Aquat. Organ.* **112**, 237-242. doi:10.3354/dao02810
Huebschman, J. J., Hoerner, S. A., White, J. P., Kaarakka, H. M., Parise, K. L. and Foster, J. T. (2019). Detection of *Pseudogymnoascus destructans* during summer on Wisconsin bats. *J. Wildl. Dis.* **55**, 673-677. doi:10.7589/2018-06-146
Jones, L. D., Cooper, R. W. and Harding, R. S. (1972). Composition of mealworm *Tenebrio molitor* larvae. *J. Zoo Anim. Med.* **3**, 34-41. doi:10.2307/20094161
Jones, K. E., Patel, N. G., Levy, M. A., Storeygard, A., Balk, D., Gittleman, J. L. and Daszak, P. (2008). Global trends in emerging infectious diseases. *Nature* **451**, 990. doi:10.1038/nature06536
Khayat, R. O. S., Shaw, K. J., Dougill, G., Melling, L. M., Ferris, G. R., Cooper, G. and Grant, R. A. (2019). Characterizing wing tears in common pipistrelles (*Pipistrellus pipistrellus*): investigating tear distribution, wing strength, and possible causes. *J. Mammal.* **100**, 1282-1294. doi:10.1093/jmammal/gyz081
Langwig, K. E., Frick, W. F., Reynolds, R., Parise, K. L., Drees, K. P., Hoyt, J. R., Cheng, T. L., Kunz, T. H., Foster, J. T. and Kilpatrick, A. M. (2015). Host and pathogen ecology drive the seasonal dynamics of a fungal disease, white-nose syndrome. *Proc. R. Soc. B* **282**, 20142335. doi:10.1098/rspb.2014.2335
Langwig, K. E., Hoyt, J. R., Parise, K. L., Frick, W. F., Foster, J. T. and Kilpatrick, A. M. (2017). Resistance in persisting bat populations after white-nose syndrome invasion. *Philos. Trans. R. Soc. B Biol. Sci.* **372**, 20160044. doi:10.1098/rstb.2016.0044
Lilley, T., Prokkola, J., Johnson, J., Rogers, E., Gronsky, S., Kurta, A., Reeder, D. and Field, K. (2017). Immune responses in hibernating little brown myotis (*Myotis lucifugus*) with white-nose syndrome. *Proc. R. Soc. B. R. Soc.* **284**, 20162232. doi:10.1098/rspb.2016.2232
Lollar, A. and French, B. A. S. (1998). *Captive Care and Medical Reference for the Rehabilitation of Insectivorous Bats*. Austin, TX: Bat Conservation International.
Lovegrove, B. G. (2009). Modification and miniaturization of Thermochron iButtons for surgical implantation into small animals. *J. Comp. Physiol. B* **179**, 451-458. doi:10.1007/s00360-008-0329-x
Marshall, K. L., Chadha, M., Sterbing-D'Angelo, S. J., Moss, C. F. and Lumpkin, E. A. (2015). Somatosensory substrates of flight control in bats. *Cell Reports* **11**, 851-858. doi:10.1016/j.celrep.2015.04.001
Martel, A., Spitzen-van der Sluijs, A., Blooi, M., Bert, W., Ducatelle, R., Fisher, M. C., Woeltjes, A., Bosman, W., Chiers, K. and Bossuyt, F. (2013). *Batrachochytrium salamandrivorans sp. nov.* causes lethal chytridiomycosis in amphibians. *Proc. Natl Acad. Sci. USA* **110**, 15325-15329. doi:10.1073/pnas.1307356110
Mayberry, H. W., McGuire, L. P. and Willis, C. K. R. (2018). Body temperatures of hibernating little brown bats reveal pronounced behavioural activity during deep torpor and suggest a fever response during white-nose syndrome. *J. Comp. Physiol. B* **188**, 333-343. doi:10.1007/s00360-017-1119-0
Meteyer, C. U., Buckles, E. L., Blehert, D. S., Hicks, A. C., Green, D. E., Shearn-Bochsler, V., Thomas, N. J., Gargas, A. and Behr, M. J. (2009). Histopathologic criteria to confirm white-nose syndrome in bats. *J. Vet. Diagn. Invest.* **21**, 411-414. doi:10.1177/104063870902100401
Meteyer, C. U., Valent, M., Kashmer, J., Buckles, E. L., Lorch, J. M., Blehert, D. S., Lollar, A., Berndt, D., Wheeler, E. and White, C. L. (2011). Recovery of little brown bats (*Myotis lucifugus*) from natural infection with *Geomyces destructans*, white-nose syndrome. *J. Wildl. Dis.* **47**, 618-626. doi:10.7589/0090-3558-47.3.618
Meteyer, C. U., Barber, D. and Mandl, J. N. (2012). Pathology in euthermic bats with white nose syndrome suggests a natural manifestation of immune reconstitution inflammatory syndrome. *Virulence* **3**, 583-588. doi:10.4161/viru.22330
Muller, L. K., Lorch, J. M., Lindner, D. L., O'Connor, M., Gargas, A. and Blehert, D. S. (2013). Bat white-nose syndrome: a real-time TaqMan polymerase chain reaction test targeting the intergenic spacer region of *Geomyces destructans*. *Mycologia* **105**, 253-259. doi:10.3852/12-242
Norquay, K. J., Martinez-Nuñez, F., Dubois, J. E., Monson, K. M. and Willis, C. K. R. (2013). Long-distance movements of little brown bats (*Myotis lucifugus*). *J. Mammal.* **94**, 506-515. doi:10.1644/12-MAMM-A-065.1
Norris, D. R. (2005). Carry-over effects and habitat quality in migratory populations. *Oikos* **109**, 178-186. doi:10.1111/j.0030-1299.2005.13671.x
O'Connor, C. M., Norris, D. R., Crossin, G. T. and Cooke, S. J. (2014). Biological carryover effects: linking common concepts and mechanisms in ecology and evolution. *Ecosphere* **5**, 1-11. doi:10.1890/ES13-00388.1
Pannkuk, E. L., Gilmore, D. F., Fuller, N. W., Savary, B. J. and Risch, T. S. (2013). Sebaceous lipid profiling of bat integumentary tissues: quantitative analysis of free fatty acids, monoacylglycerides, squalene, and sterols. *Chem. Biodivers.* **10**, 2122-2132. doi:10.1002/cbdv.201300319
Pannkuk, E., Fuller, N., Moore, P., Gilmore, D., Savary, B. and Risch, T. (2014). Fatty acid methyl ester profiles of bat wing surface lipids. *Lipids* **49**, 1143-1150. doi:10.1007/s11745-014-3951-2
Pannkuk, E. L., McGuire, L. P., Warnecke, L., Turner, J. M., Willis, C. K. and Risch, T. S. (2015). Glycerophospholipid profiles of bats with white-nose syndrome. *Physiol. Biochem. Zool.* **88**, 425-432. doi:10.1086/681931
Pappas, A. (2009). Epidermal surface lipids. *Dermatoendocrinology* **1**, 72-76. doi:10.4161/derm.1.2.7811
Parris, M. J. and Beaudoin, J. G. (2004). Chytridiomycosis impacts predator-prey interactions in larval amphibian communities. *Oecologia* **140**, 626-632. doi:10.1007/s00442-004-1631-2
Peckarsky, B. L., Cowan, C. A., Penton, M. A. and Anderson, C. (1993). Sublethal consequences of stream-dwelling predatory stoneflies on mayfly growth and fecundity. *Ecology* **74**, 1836-1846. doi:10.2307/1939941
Pollock, T., Moreno, C. R., Sánchez, L., Ceballos-Vasquez, A., Faure, P. A. and Mora, E. C. (2015). Wound healing in the flight membranes of wild big brown bats. *J. Wildl. Manag.* **80**, 19-26. doi:10.1002/jwmg.997
Prendergast, B., Freeman, D., Zucker, I. and Nelson, R. (2002). Periodic arousal from hibernation is necessary for initiation of immune response in ground squirrels. *Am. J. Physiol. Regul. Integr. Comp. Physiol.* **282**, R1054-R1062. doi:10.1152/ajpregu.00562.2001
Racey, P. A. (1970). The breeding, care and management of vespertilionid bats in the laboratory. *Lab. Anim.* **4**, 171-183. doi:10.1258/002367770781071635
Racey, P. A. (1982). Ecology of bat reproduction. In *Ecology of Bats* (ed. T. H. Kunz), pp. 57-104. Boston, MA: Springer.
Racey, P. A. and Swift, S. M. (1981). Variations in gestation length in a colony of pipistrelle bats (*Pipistrellus pipistrellus*) from year to year. *Reproduction* **61**, 123-129. doi:10.1530/jrf.0.0610123
Reeder, D. M., Frank, C. L., Turner, G. G., Meteyer, C. U., Kurta, A., Britzke, E. R., Vodzak, M. E., Darling, S. R., Stihler, C. W. and Hicks, A. C. (2012). Frequent arousal from hibernation linked to severity of infection and mortality in bats with white-nose syndrome. *PLoS ONE* **7**, e38920. doi:10.1371/journal.pone.0038920
Reichard, J. D. and Kunz, T. H. (2009). White-nose syndrome inflicts lasting injuries to the wings of little brown myotis (*Myotis lucifugus*). *Acta Chiropt.* **11**, 457-464. doi:10.3161/150811009X485684
Reichard, J. D., Fuller, N. W., Bennett, A. B., Darling, S. R., Moore, M. S., Langwig, K. E., Preston, E. D., Oettingen, S. V., Richardson, C. S. and Scott Reynolds, D. (2014). Interannual survival of *Myotis lucifugus* (Chiroptera: Vespertilionidae) near the epicenter of white-nose syndrome. *Northeast. Nat.* **21**, N56-N59. doi:10.1656/045.021.0410
Rosenblum, E. B., Voyles, J., Poorten, T. J. and Stajich, J. E. (2010). The deadly chytrid fungus: a story of an emerging pathogen. *PLoS Pathog.* **6**, e1000550. doi:10.1371/journal.ppat.1000550
Schneider, C. A., Rasband, W. S. and Eliceiri, K. W. (2012). NIH Image to ImageJ: 25 years of image analysis. *Nat. Methods* **9**, 671. doi:10.1038/nmeth.2089
Sheriff, M. J., Krebs, C. J. and Boonstra, R. (2009). The sensitive hare: sublethal effects of predator stress on reproduction in snowshoe hares. *J. Anim. Ecol.* **78**, 1249-1258. doi:10.1111/j.1365-2656.2009.01552.x
Smith, J. A. (1994). Neutrophils, host defense, and inflammation: a double-edged sword. *J. Leuko. Biol.* **56**, 672-686.
Speakman, J. and Thomas, D. (2003). *Physiological ecology and energetics of bats*. In *Bat Ecology* (ed. T. H. Kunz and M. B. Fenton), pp. 430-490. Chicago, IL: Chicago University Press.
Sterbing-D'Angelo, S., Chadha, M., Chiu, C., Falk, B., Xian, W., Barcelo, J., Zook, J. M. and Moss, C. F. (2011). Bat wing sensors support flight control. *Proc. Natl. Acad. Sci.* **108**, 11291-11296. doi:10.1073/pnas.1018740108
Stones, R. C. and Wiebers, J. E. (1965). Seasonal changes in food consumption of little brown bats held in captivity at a "neutral" temperature of 92°F. *J. Mammal.* **46**, 18-22.
Turner, G. G., Meteyer, C. U., Barton, H., Gumbs, J. F., Reeder, D. M., Overton, B., Bandouchova, H., Bartonicka, T., Martínková, N. and Pikula, J. (2014). Nonlethal screening of bat-wing skin with the use of ultraviolet fluorescence to detect lesions indicative of white-nose syndrome. *J. Wildl. Dis.* **50**, 566-573. doi:10.7589/2014-03-058
Vander Wal, E., Garant, D., Festa-Bianchet, M. and Pelletier, F. (2013). Evolutionary rescue in vertebrates: evidence, applications and uncertainty. *Philos. Trans. R. Soc. B Biol. Sci.* **368**, 20120090. doi:10.1098/rstb.2012.0090
Venesky, M. D., Parris, M. J. and Storfer, A. (2009). Impacts of *Batrachochytrium dendrobatidis* infection on tadpole foraging performance. *Ecohealth* **6**, 565-575. doi:10.1007/s10393-009-0272-7
Verant, M. L., Carol, M. U., Speakman, J. R., Cryan, P. M., Lorch, J. M. and Blehert, D. S. (2014). White-nose syndrome initiates a cascade of physiologic disturbances in the hibernating bat host. *BMC Physiol.* **14**, 10. doi:10.1186/s12899-014-0010-4
Voigt, C. C. (2013). Bat flight with bad wings: is flight metabolism affected by damaged wings? *J. Exp. Biol.* **216**, 1516-1521. doi:10.1242/jeb.079509
Voyles, J., Young, S., Berger, L., Campbell, C., Voyles, W., Dinudom, A., Cook, D., Webb, R., Alford, R., Skerratt, L. et al. (2009). Pathogenesis of chytridiomycosis, a cause of catastrophic amphibian declines. *Science* **326**, 582-585. doi:10.1126/science.1176765
Warnecke, L., Turner, J. M. and Geiser, F. (2008). Torpor and basking in a small arid zone marsupial. *Naturwissenschaften* **95**, 73-78. doi:10.1007/s00114-007-0293-4

Warnecke, L., Turner, J. M., Bollinger, T. K., Lorch, J. M., Misra, V., Cryan, P. M., Wibbelt, G., Blehert, D. S. and Willis, C. K. R. (2012). Inoculation of bats with European *Geomyces destructans* supports the novel pathogen hypothesis for the origin of white-nose syndrome. *Proc. Natl. Acad. Sci. USA* **109**, 6999-7003. doi:10.1073/pnas.1200374109

Warnecke, L., Turner, J. M., Bollinger, T. K., Misra, V., Cryan, P. M., Blehert, D. S., Wibbelt, G. and Willis, C. K. (2013). Pathophysiology of white-nose syndrome in bats: a mechanistic model linking wing damage to mortality. *Biol. Lett.* **9**, 20130177. doi:10.1098/rsbl.2013.0177

Weaver, K. N., Alfano, S. E., Kronquist, A. R. and Reeder, D. M. (2009). Healing rates of wing punch wounds in free-ranging little brown myotis (*Myotis lucifugus*). *Acta Chiropt.* **11**, 220-223. doi:10.3161/150811009X465866

Wilcox, A. and Willis, C. K. (2016). Energetic benefits of enhanced summer roosting habitat for little brown bats (*Myotis lucifugus*) recovering from white-nose syndrome. *Conser. Physiol.* **4**, cov070. doi:10.1093/conphys/cov070

Willis, C. K. (2015). Conservation physiology and conservation pathogens: white-nose syndrome and integrative biology for host–pathogen systems. *Integr. Comp. Biol.* **55**, 631-641. doi:10.1093/icb/icv099

Willis, C. K. and Brigham, R. M. (2007). Social thermoregulation exerts more influence than microclimate on forest roost preferences by a cavity-dwelling bat. *Behav. Ecol. Sociobiol.* **62**, 97-108. doi:10.1007/s00265-007-0442-y

Ziboh, V. A., Miller, C. C. and Cho, Y. (2000). Metabolism of polyunsaturated fatty acids by skin epidermal enzymes: generation of antiinflammatory and antiproliferative metabolites. *Am. J. Clin. Nutr.* **71**, 361s-366s. doi:10.1093/ajcn/71.1.361s

Table S1. Principle component analysis of fatty acids (FA) taken from the skin surface of recovering little brown bats. The first principal component represents FA saturation, while the second reflects carbon chain length.

Fatty Acid Type	***PC1 (Saturation)***	***PC2 (Chain Length)***	***Proportion at capture***	***Proportion at day 40***	***Change***
Palmitic acid (16:0)	0.200	-0.607	0.159	0.157	-0.002
Stearic acid (18:0)	0.375	-0.285	0.218	0.290	0.072
Oleic acid (18:1)	-0.390	-0.094	0.214	0.113	-0.101
Linoleic acid (18:2)	-0.413	0.051	0.219	0.120	-0.100
α-linoleic acid (18:3)	-0.372	0.1685	0.037	0.013	-0.023
Arachidic acid (20:0)	0.341	0.254	0.020	0.030	0.010
Gondoic acid (20:1)	0.021	0.561	0.015	0.020	0.005
Heneicosylic acid (21:0)	0.345	0.258	0.028	0.126	0.099
Lignoceric acid (24:0)	0.348	0.253	0.055	0.097	0.042
Proportion of total variance explained	0.618	0.206	-	-	-

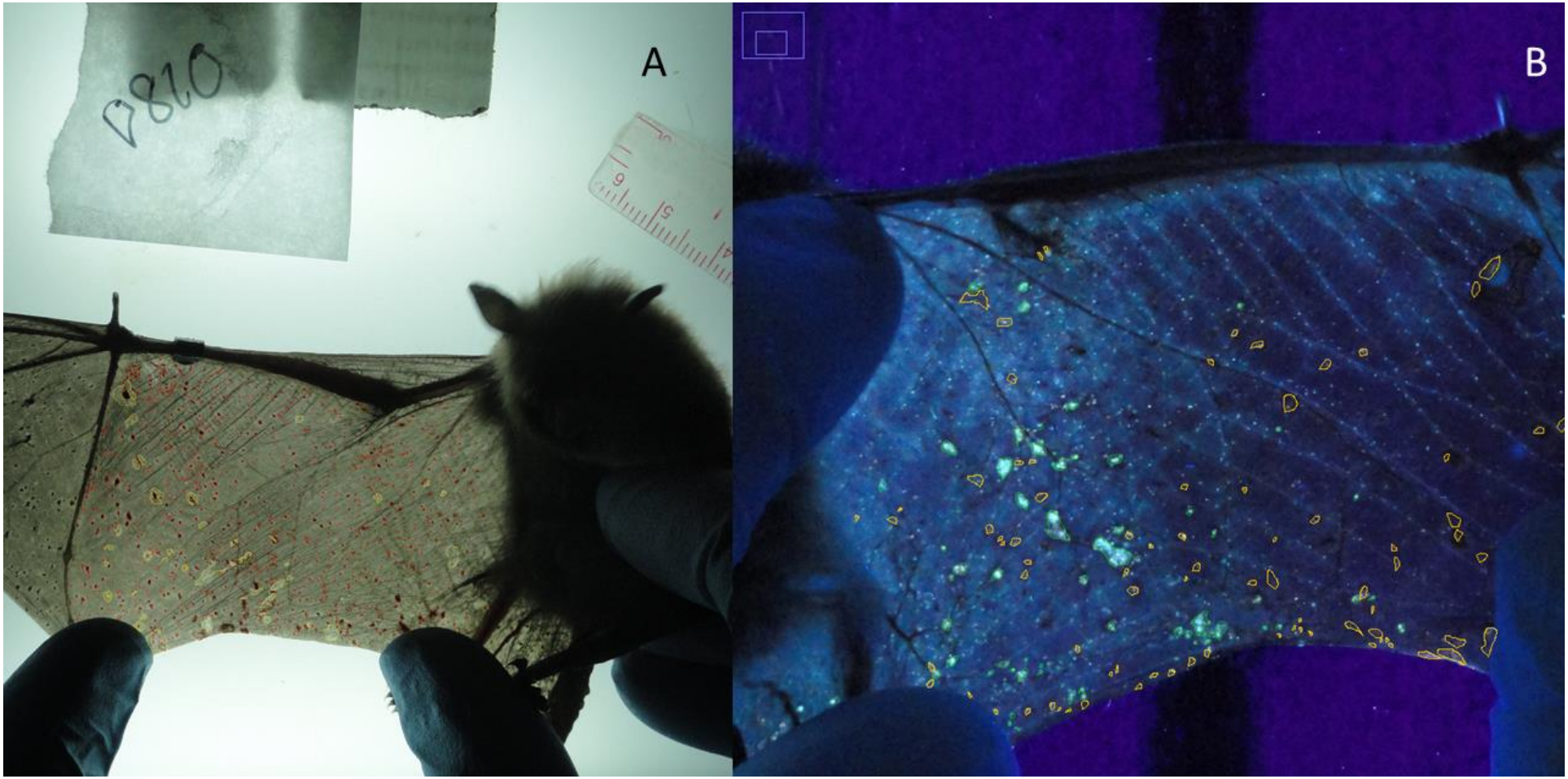

Figure S1. An example of white discoloration (highlighted in yellow), black spots (highlighted in red), teal fluorescence (highlighted in green), and orange fluorescence (highlighted in orange). Lesion counts and estimated area of wing damage were calculated from these selections.

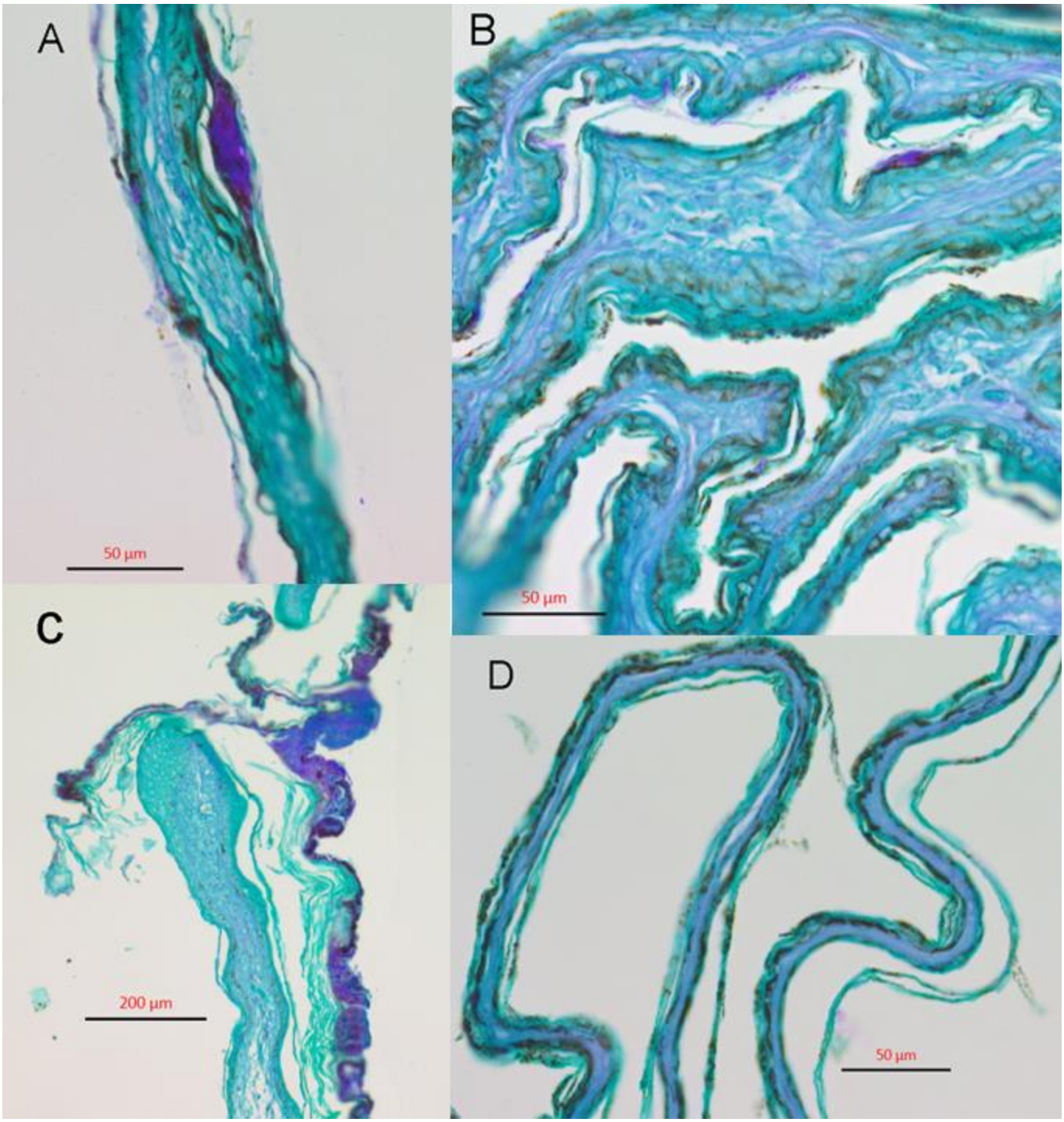

Figure S2. Examples of histopathological sections taken from bats during healing. At days 5 – 7, fungal elements (magenta portions on skin surface) are present throughout the sections, along with clusters of hyphae and inflammatory crusts (A). After two weeks of healing, fungal elements are less prevalent and skin structure resembles that of normal tissue (B). At this time, holes caused by fungal action begin to grow shut, as epithelial cells proliferate at the wound margins and surface crusts slough from the wing surface (C). By day 40 of this study, wing tissue is indistinguishable from that of uninfected bats and fungal elements are not observed (D).